

See discussions, stats, and author profiles for this publication at: <https://www.researchgate.net/publication/51956696>

Shock-Generated Turbulence In the Innermost 50 pc of the Galaxy Center

Article · November 2011

DOI: 10.1063/1.3701362 · Source: arXiv

CITATIONS

2

READS

113

2 authors, including:



Itzhak Goldman

Afeke Tel-Aviv Academic College of Engineering

91 PUBLICATIONS 1,490 CITATIONS

SEE PROFILE

Some of the authors of this publication are also working on these related projects:



Giant Molecular Clouds and modified gravity [View project](#)



pulsar scintillations and extremely thin scattering screens in the local ISM [View project](#)

Shock-Generated Turbulence In the Innermost 50 pc of the Galaxy Center

Itzhak Goldman^{*,†} and Marcella Contini[†]

**Department of Exact Sciences, Afeka Tel Aviv Academic College of Engineering
Tel Aviv 69107, Israel*

*†School of Physics and Astronomy, Department of Astronomy and Astrophysics, Tel Aviv University
Tel Aviv 69978, Israel*

Abstract. The center of the Milky Way galaxy (MW) is an extreme environment which contains a massive black hole surrounded by a very dense star cluster, two other adjacent star clusters, and a giant molecular cloud which would serve as an incubator to a new generation of stars. The gas and dust in its vicinity are denser by 2-3 orders of magnitude than in other locations in the MW. This is also the case with the magnetic field. The kinematics of the gas is characterized by apparently random, supersonic flows. In this paper we provide observational evidence for the existence of a supersonic turbulence, most likely generated by the shock waves. Moreover, the mere existence of turbulence and its characteristics are shown to be instrumental in testing the validity and consistency of theoretical modeling of the spectra of the gas filaments.

Keywords: Galaxy:center-Galaxy: kinematics and dynamics-Galaxy:ISM-turbulence

PACS: 98.35.Jk, 98.38.-j, 47.27.tb

INTRODUCTION

The center of the Milky Way galaxy (MW) is an extreme environment, very different from the other locations in the MW. It contains a dormant $\sim 4 \times 10^6 M_{\odot}$ black hole, three massive clusters of young high-mass stars and a giant molecular cloud (see reviews in [1]). The densities of gas and dust are 2-3 orders of magnitudes higher than the Galactic average, the magnetic field is in the range of $(100 \div 1000) \mu G$, while the Galactic norm is few μG . The gas exhibits a complex filamentary morphology as well as a supersonic velocity field.

The GC has been observed in infrared and radio bands because the high gas and dust densities combined with a line of sight to the Galactic center (GC) that passes through the MW disk, strongly absorb optical and UV radiation. Infrared telescopes have advanced considerably in the past decades; the Spitzer infrared space telescope is the most recent and advanced infrared facility to date. The left panel of Figure 1 is an artist concept of the Spitzer telescope while the right one is the Spitzer image (in 3 mid-infrared wavelengths) of a ~ 600 pc extent of the MW disk around the GC.

Zooming in, Figure 2 which is adapted from [2], shows the inner 50 pc of the GC. The

¹ Talk presented by Itzhak Goldman

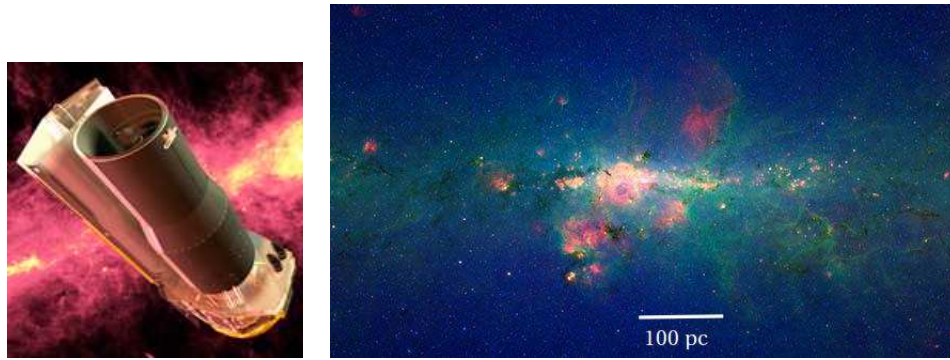


FIGURE 1. **left:** Spitzer Telescope—artist concept. **right:** Spitzer image of the Galactic center region. *blue:* $3.6 \mu\text{m}$, *green:* $8 \mu\text{m}$, *red:* $24 \mu\text{m}$. The brightest white feature at the center of the image is the central star cluster in our galaxy, surrounding the massive black hole. *source:* Spitzer website.

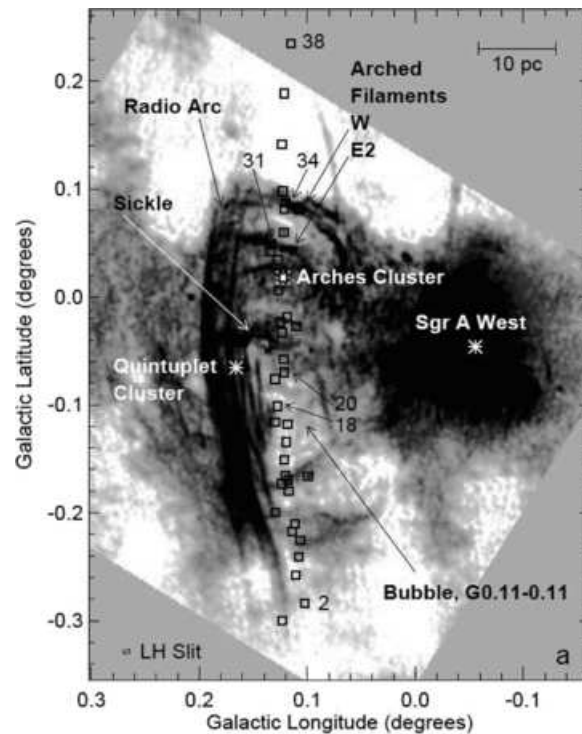


FIGURE 2. A 21 cm radio continuum (log-log scale) image [3] with 11 arcsec resolution. Except for the Radio Arc and part of the Sgr A region which are non-thermal, all the radio emission is thermal bremsstrahlung. The 38 positions observed by with the Spitzer telescope in the mid- infrared [2] are indicated by square boxes. (adapted from Fig. 1 of [2])

black hole Sgr A West is surrounded by the nuclear star cluster (not marked in the figure). At a distance of about 25 pc in the Galactic plane are the Quintet and the Arches star clusters. Most of the stars are young (age ~ 2 Myr) and massive ($10 - 50 M_{\odot}$). Visible in the images are the Arches and the Sickle gas filaments. Visible also is a system of quasi circular arcs whose morphologies suggest that they were formed by stellar winds

(velocities ~ 1000 km/s) emanating from the Quintet and the Arches star clusters.

Observations with the Spitzer Telescope by [2] yielded high quality mid-infrared spectra at 38 positions along a line perpendicular to the MW disk (the positions are marked by the squares in Figure 2). The observational spectra lead to the conclusion that the gas in the filaments is indeed excited by ionizing UV photons originating in the adjacent star clusters [2]. However, photo-ionization by itself cannot account for the observed line ratios and an additional excitation by shocks is probably important. Shocks are indeed expected since the line of sight (radial) gas velocities measured by radio observations ([4, 5]) span a range of 180 km/s. Moreover, the filamentary fractured structure of the gas can be naturally explained as the result of turbulence generated by shocks.

Following on this proposition, a detailed modeling of the line and continuum spectra allowing for both photo-ionization and shocks as the sources of excitation has been carried out [6]. All the available lines in each spectrum and the continuum spectral energy distribution were modeled consistently. Indeed, this modeling reproduced correctly the observational spectra and at the same time was able to derive the shock velocity, pre-shock density and magnetic field, and the geometrical depth at each of the 38 positions. More recently [7], these values of the physical parameters have been used to calculate the expected spectra in the optical and UV ranges, which cannot be observed by the presently available instruments.

OUTLINE

The analysis presented in [6] invoked the existence of shocks as a necessary ingredient for the consistent derivation of the spectra observed by [2]. Shocks are known to produce turbulence, notably via the Richtmyer-Meshkov instability ([8], [9]) which is due to the shock acceleration, and is similar to the familiar Raleigh-Taylor instability. Shocks can also excite turbulence by creating flows that exhibit shear instability or Kelvin Helmholtz instability which in turn generate turbulence. Indeed, the clumped and fragmented morphology of the region strongly suggests the existence of an underlying supersonic shock-generated turbulence.

The existence of turbulence can be probed directly by analyzing the velocity spectrum. In addition, the imprint of turbulence may be detected indirectly by analyzing the power spectrum of "passive scalars"([10]), which are strongly coupled to the gas and follow its turbulent motion (but do not feed-back on the turbulence). The power spectrum of a passive scalar is proportional to that of the turbulent velocity.

An example is the 21 cm emissivity which is proportional to the column density of the neutral hydrogen and its fluctuations reflect the density fluctuations and in turn the velocity fluctuations. In the case of infrared continuum the passive scalar is the dust density, and in the case of abundances it is the concentration of the species under consideration.

The observational power spectrum of a passive scalar provides a measure of its hierarchical spatial structure. When this power spectrum is a power law, a hydro-turbulence is naturally suggested as the mechanism that has shaped the observed spatial hierarchy. Yet, by itself, such a spectrum is not enough to prove the existence of a hydrodynamical

turbulence. On the other hand, if the power spectrum of the velocity field reveals a turbulence, the fact that the power spectrum of a passive scalar is also a power law with the same exponent strengthens the case for the reality of the velocity turbulence.

An example is the power spectrum of 21cm emission in the Small Magellanic Cloud (SMC) [11]. It was shown by [12] that the power spectrum is consistent with that generated by a large scale velocity turbulence. Additional support for the existence of a dynamic turbulence was obtained by [13] by deriving the power spectrum of the radial velocities of the giant H_I super-shells of the SMC and showing that the two power spectra are consistent.

In what follows we analyze the radial velocity data of [2] and their observed mid-IR continuum flux in order to test for the existence of turbulence. Indeed these two kinds of observational data reveal the existence of a supersonic turbulence.

Following these two analyses, we examine the Si/H abundance ratio as function of position which were *computed* by [6]. The idea being that if these computations indeed reproduce the actual physical conditions in the region, then the imprint of the turbulence should be evident in the computed abundance as function of position. It turns out to be indeed the case; thus lending credibility to the computations of [6] as well as to, their extensions to the optical and UV ranges [7]. Finally, we estimate the effect of turbulence on the magnetic field in the observed positions.

TURBULENCE: RADIAL VELOCITIES

The 3D spectral function of the turbulent velocity, $\Phi(\vec{k})$ is defined in terms of the 2-point autocorrelation of the turbulent velocity field

$$\langle \vec{v}(\vec{r}') \cdot \vec{v}(\vec{r} + \vec{r}') \rangle = \int \Phi(\vec{k}) e^{i\vec{k} \cdot \vec{r}} d^3k$$

In the homogeneous and isotropic case it is useful to introduce the turbulence energy spectrum $E(k)$ and the turbulent velocity spectral function $F(k) = 2E(k)$ so that

$$\Phi(\vec{k}) = \Phi(k) = \frac{F(k)}{4\pi k^2}; k = |\vec{k}|$$

Assuming the ergodic principle, ensemble averages can be replaced by space, surface, or as in the present case, line averages.

The assumed isotropy implies that $F_r(k)$, - the power spectrum of the radial turbulent velocity is

$$F_r(k) = \frac{1}{3}F(k)$$

and can be derived from

$$\langle v_r(x')v_r(x' + x) \rangle = \frac{1}{L} \int_0^L v_r(x')v_r(x' + x)dx = \frac{1}{2\pi} \int_0^L F_r(k)e^{ikx}dk$$

where L is the length of the line along which the radial velocity has been measured. The power spectrum thus is the one dimensional Fourier transform of the 2-point autocorre-

lation function of the radial velocity. Since the data are given at a set of discrete positions we compute the power spectrum by employing a digital Fourier transform. Note that at each position the mean squared turbulent radial velocity

$$\langle v_r^2 \rangle = \frac{1}{2\pi} \int_0^L F_r(k) dk$$

is contributed by all the spatial scales of the spectrum.

The observational data are given for 38 positions along an almost straight line with extension of about 75 pc [2]. Not all positions are evenly spaced, thus a numerical uncertainty in the small-scales part of the power spectrum is expected.

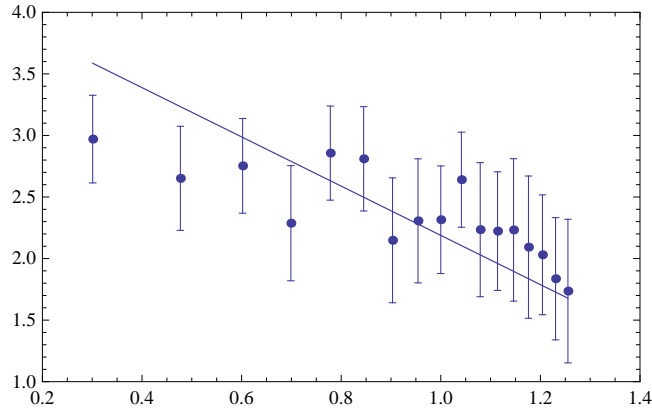


FIGURE 3. The power spectrum of the radial velocity residuals, in units of $(\text{km/s})^2$, as function of the relative wavenumber k . $k = 1$ corresponds to the spatial scale $l_0 = 75 \text{ pc}$. The line is a power law with index -2 .

Also, the radial velocity observed by [2] for the m20 position is substantially larger than the adjacent velocities and most likely is a foreground flow. We therefore adopt for this point a value equal to the mean velocity of the other positions.

If the residual velocities were random *uncorrelated* fluctuation the power spectrum would have been a "white noise" with the same power on all wavelengths. In contrast, the power spectrum shown in Figure 3 is a rather steep decreasing function of the wavenumber k . The largest turbulence scale corresponding to the dimensionless wavenumber $k = 1$ is the linear extent of the data strip: $l_0 = 75 \text{ pc}$. The value of the root mean squared turbulent radial velocity at the largest scale is $v_0 = 17.4 \text{ km/s}$ corresponding to a 3D velocity of 30 km/s , well above the thermal velocity of $\sim 10 \text{ km/s}$.

The line in the figure is a k^{-2} power law that is expected for supersonic turbulence ([14], [15]). It differs from $k^{-5/3}$ Kolmogorov spectrum which characterizes incompressible turbulence. The steeper slope is due to the fact that a fraction of the turbulent kinetic energy density is converted to compression work and is diverted from the energy cascaded to the smaller spatial scales.

In order to obtain a quantitative estimate of the goodness of the fit we adopted the uncertainty of 15 km/s for each individual measurement [2]. Then we obtained synthetic velocity data by generating at each position a random velocity using a normal distribution with a mean equal to the observed value, and a standard deviation of 15 km/s .

We have generated 100 such simulated data sets. For each, the power spectrum was computed enabling an estimate for the standard deviation of the power spectrum.

Doing so, a value of 0.72 was obtained for the reduced χ^2 . Some of the uncertainty in the power spectrum stems from the uneven spacing of the positions leading to a scatter in the power spectrum at the small spatial scales (large k). The fact that even so the fit is a good one suggests that the true uncertainty in the observed velocities is *smaller* than the assumed value of 15 km/s.

The characteristic timescale of the turbulence is given by $\tau_0 \sim l_0/v_0 \sim 4 \times 10^6$ yr – comparable to the age of the young stellar populations. This is consistent with the framework adopted in [2] and [6] that stellar outflows are the main energy source that shaped the interstellar medium in this region and together with the stellar UV radiation are also responsible for the observed mid-infrared spectra.

The derived power spectrum seems to steepen to a k^{-3} dependence at about $k = 7$. If real, it implies that geometrical depth along the radial line of sight is about $\frac{1}{15}$ of the extent on the plane of the sky ([12]); namely a depth of ~ 5 pc.

TURBULENCE: MID-IR FLUX

The observed flux is an integral of the emissions along the line of sight. In the optically thin case it is contributed by all the geometrical depth along the line of sight while in the optically thick case only the foreground layers contribute. Recently, [16, 17] have studied fluctuations of the far-IR continuum flux from thermally heated dust and concluded that their power spectrum is identical to that of the underlying velocity turbulence. The interpretation of this result was that the dust is strongly coupled to the gas and thus the dust density fluctuations are determined by the gas velocity field which is turbulent. In the cases considered by these authors the turbulence was subsonic and the power spectrum was the Kolmogorov spectrum.

Pursuing a similar analysis, we compute the power spectrum of the fluctuations of the mid-IR continuum flux in the range $(13.5 - 14.3)\mu m$, as function of position. Mathematically, the procedure is the same employed in the previous section with regard to the radial velocity.

The resulting power spectrum is displayed in Figure 4. It exhibits a clear k^{-2} behavior for the larger scales and an indication of a possible steepening at about $k = 7$ to a k^{-3} dependence; in effect the latter is more obvious here than in the radial velocity spectrum.

The uncertainties reported by [2] are quite small (of the order of 1%). As a result the uncertainties in the power spectrum are too small to be indicated in the figure. The scatter in the power spectrum is dominated by the uneven spacing of the positions [2]. The latter can be estimated by generating synthetic data with randomly spacings (much in the way as with the velocity uncertainties in the previous section), However this seems to be outside the scope of the present paper. Therefore, we do not derive here a quantitative estimate for the goodness of fit. Rather we would like to draw attention to the fact that the deviations from the power law are mostly at the small spatial scales, as expected from an uneven spacing, and not on the large scales.

The important conclusion from this power spectrum is that it is consistent with the interpretation that the dust density fluctuations (responsible for the flux fluctuations)

were driven by the supersonic velocity turbulence addressed in the previous section.

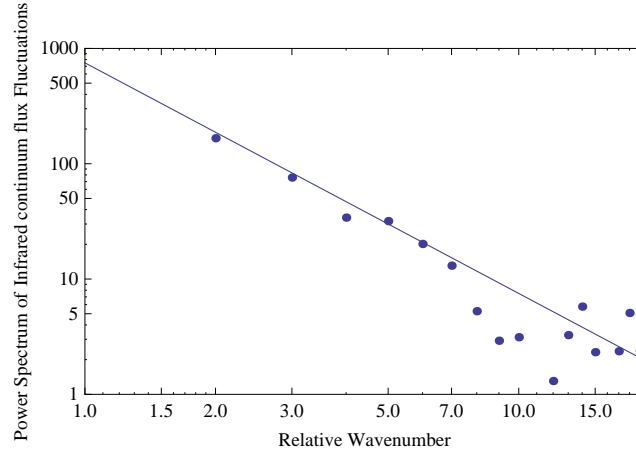


FIGURE 4. The power spectrum of the mid-IR continuum at $(13.5 - 14.3)\mu m$, in units of Jy^2 , as function of the relative wavenumber k . $k = 1$ corresponds to the spatial scale $l_0 = 75pc$. The line is a power law with index -2 .

TURBULENCE: SI/H ABUNDANCE RATIO

In [6] various abundance ratios were computed as function of position. If these computations are a fair representation of the physics in the region, it is expected that the computed abundances will reflect the turbulence revealed in the observational radial velocity and mid-IR flux.

If the heavy elements, whose abundance is considered, are strongly coupled to the gas and follow the gas motions then they can be regarded as a turbulent "passive scalars" ([10]), much in the same way as the dust density responsible for the mid-IR emission. As in the latter case, the power spectrum should be proportional to the turbulent velocity power spectrum. We computed the power spectrum of the fluctuations of the Si/H ratio at the 38 positions mentioned in the previous sections. This specific abundance was selected because it does not show drastic variations with position and thus (unlike as with e.g. Fe/H) the fluctuations are not affected by trapping into dust grains and eventual sputtering.

The resulting power spectrum is shown in Figure 5. The uncertainties in the power spectrum resulting from the uncertainties of the computed abundance are too small to be indicated in the figure. The scatter seen in the small scales (large wavenumbers) probably reflects the uneven spacing of the observational positions. The power spectrum is consistent with the k^{-2} spectrum of the radial velocity turbulence and that of the mid-IR flux. The consistency of the power spectrum with what is expected from an underlying supersonic hydrodynamic turbulence strengthens the case for the existence of the latter. More importantly, this lends credibility to the computational model employed in [6]. Here, too there is an indication for a steepening of the spectrum at $k \sim 7$ to a k^{-3} dependence.

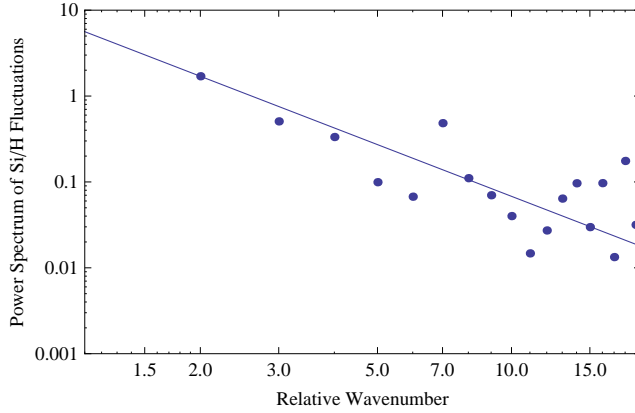


FIGURE 5. The power spectrum of Si/H residuals, in units of 10^{-10} , as function of the relative wavenumber k . $k = 1$ corresponds to the spatial scale $l_0 = 75pc$. The line is a power law with index -2 .

DISCUSSION

The clumped and fragmented morphology of the GC region strongly suggests that it has been shaped by a supersonic turbulence. The latter has been generated by shocks driven by the high velocity stellar winds from the young massive stars located in the adjacent star clusters. Shocks are known to produce turbulence directly, via the Richtmyer-Meshkov instability due to the shock acceleration, and also indirectly by giving rise to shear and Kelvin Helmholtz instabilities which in turn excite turbulence.

The existence of such a turbulence was revealed in the power spectra of the observational radial velocities and mid-IR continuum flux. The power spectra exhibit a k^{-2} behavior typical to supersonic turbulence, and is steeper than the Kolmogorov spectrum that corresponds to incompressible turbulence. A steepening of the power spectra for relative wave numbers exceeding 7, suggests that the line of sight depth of the turbulent region is about 5pc. The turbulence radial root mean squared velocity is about 17 km/s and its 3D value is about 30 km/s indicating a turbulence Mach number of about 2-3. The associated turbulence timescale is about 4 Myr – comparable to the age of the young stellar populations which are ultimate generators of the shocks and the ensuing turbulence. Since the modeling of the observed mid infrared spectra [6] invokes the existence of shocks – our finding lends credibility to the latter assumption. The models also predict the abundances as function of position [6]. Analysis of the Si/H abundance field, reveals the same underlying turbulence as do the observational velocities and the mid-infrared flux. This implies that the modeling of [6] does indeed reproduces the true physical parameters of the gas.

The turbulence can amplify the initial magnetic fields [6] up to equipartition value if the available time is much larger than the turbulence timescale. The amplification proceeds via the dynamo mechanism involving the winding up of magnetic field flux lines by the turbulence eddies.

For the 3D turbulent velocity of 30 km/s, the equipartition value for the largest scale is $B_{turb,eq} = 140\mu G (n/100cm^{-3})^{1/2}$ with n denoting the gas number density.

Fields of this strength and even an order of magnitude higher were reported for the Galactic center region (see review by [?]). The larger fields could have evolved from the turbulently amplified field by an inverse cascade process ([19]) from small to large spatial scales, or directly by shock compression of the magnetic flux lines embedded in the ionized ISM [20].

ACKNOWLEDGMENTS

Itzhak Goldman thanks Michael Mond and Pierre-Louis Sulem for the invitation to the interesting and well organized WISAP-2011 conference in Eilat. He also wishes to thank the Afeka College Research Authority for financial support.

REFERENCES

1. R. Schödel, G. C. Bower, M. P. Muno, S. Nayakshin, and T. Ott *Journal of Physics Conference Series* **54**, (2006). *Electronic version*: <http://iopscience.iop.org/1742-6596/54/1>
2. Simpson, J. P., S. W. J. Colgan, A. S. Cotera, E. F. Erickson, D. J. Hollenbach, M. J. Kaufman, and R. H. Rubin *ApJ*, **670**, 1115 (2007).
3. Yusef-Zadeh, F. and M. Morris *ApJ*, **320**, 545 (1987).
4. F. Yusef-Zadeh, D. A. Roberts, and M. Wardle *ApJ*, **490**, L83 (1997).
5. C. C. Lang, K. E. Johnson, W. M. Goss, and L. F. Rodríguez *AJ*, **130**, 2185 (2005).
6. M. Contini, *MNRAS*, **399**, 1175 (2009).
7. M. Contini, and I. Goldman *MNRAS*, **411**, 792 (2011).
8. K. O. Mikaelian, *Physics of Fluids*, **2**, 592 (1990).
9. M. J. Graham, and Q. Zhang *APJS*, **127**, 339 (2000).
10. M. Lesieur, *Turbulence in Fluids* (Dordrecht: Kluwer), 6.1 (1997).
11. S. Stanimirovic, L. Staveley-Smith, J. M. Dickey, R. J. Sault, and S. L. Snowden *MNRAS*, **302**, 417 (1999).
12. I. Goldman, *ApJ*, **541**, 701 (2000).
13. I. Goldman, *IAU Symposium*, **237**, 96 (2007).
14. Passot, T., A. Pouquet, and P. Woodward *A & A*, **197**, 228 (1988).
15. Girimaji, S. S. and Y. Zhou *Phys. Lett. A*, **202**, 279 (1995).
16. M.-A. Miville-Deschênes, G. Lagache, F. Boulanger, and J.-L. Puget *A & A*, **469**, 595 (2007).
17. , M.-A. Miville-Deschênes, and 45 colleagues *A & A*, **518**, L104 (2010).
18. J. P. Vallée *New Astronomy Review*, **48**, 763 (2004).
19. P. D. Mininni, *PRE*, **76**, 026316 (2007).
20. M. V. Medvedev, L. O. Silva, and M. Kamionkowski in *Turbulence and Nonlinear Processes in Astrophysical Plasmas, AIPC*, **932**, 117 (2007).